Reactive Compatibilization of PA 6/ABS Blends by Ethylene-Acrylate-Glycidyl Methacrylate Copolymer

Bofen Huang, Dan Li, Zhiyuan Li, Xiao Li, Weihua Zhou

School of Material Science and Engineering, Nanchang University, Xuefu Road, Nanchang 330031, People's Republic of China

Received 25 August 2010; accepted 10 January 2011
DOI 10.1002/app.34160
Published online 4 May 2011 in Wiley Online Library (wileyonlinelibrary.com).

ABSTRACT: The polyamide 6/acrylonitrile-butylene-styrene copolymer (PA 6/ABS) blends were prepared using the twin-screw extruder with ethylene-acrylate-glycidyl methacrylate copolymer (EAGMA) as the reactive compatibilizer. The structure, morphology, thermal, and mechanical properties of the blends were carefully investigated. The results indicated that the ring-opening reaction of epoxy groups of EAGMA in the presence of amine and carboxyl groups of PA 6 led to the formation of EAGMA grafted PA 6 copolymer. The grafted copolymer serving as the compatibilizer eventually led to the decrease of the phase diameters as observed from the scanning electron microscope (SEM). The crystallization and melting behavior of PA 6 were restricted by the incorporation of both ABS and EAGMA, and the addition of EAGMA improved the thermal stability of the PA 6/ABS blends. Heat deformation temperature (HDT) of the blends reached a maximum value at EAGMA content of 12 wt %, which is about 45°C above the HDT of pristine PA 6. The tensile strength of the blends decreased with an increasing EAGMA content, and the impact strength of the blends showed the highest value at EAGMA content of 20 wt %, which is about 323% higher than that of pristine PA 6.
 J Appl Polym Sci 122: 586–592, 2011

Key words: polyamide 6; ABS; ethylene-acrylate-glycidyl methacrylate copolymer; reactive compatibilization

INTRODUCTION

Blending of polymers with different physical properties presents the possibility of enhancing the overall properties of a material through a synergistic combination of the desirable properties of each component in one system. However, the immiscibility of most polymers leads to the formation of multiple phase structures, which determines the properties of the resulting materials.[1–3] Different types of compatibilizers have been developed to reduce the phase separation and improve the properties of the blends.[4]

Polyamide 6 (PA 6) is a semi-crystalline thermoplastic, showing a strong chemical resistance to organic solvents, excellent mechanical performance, and adequate melt viscosity under processing conditions.[5] However, the high sensitivity to notch propagation under impact test, the high moisture sorption, and the poor dimensional stability restrict the application of PA 6 in more diverse fields. The acrylonitrile-butadiene-styrene copolymer (ABS) consists of butadiene rubber dispersed in a matrix of styrene-acrylonitrile copolymer (SAN), exhibiting excellent impact strength at low temperatures and low sensitivity to notch propagation.[6] Blends of PA 6 and ABS are of significant commercial interest. However, pristine PA 6/ABS blends exhibit an obvious phase separation and poor mechanical properties. Compatibilization is therefore a potential method of obtaining blends.[7,8]

PA 6 contains amine and carboxyl groups at the ends of the polymer chains, and these groups will react with other groups during the extruding process. Therefore, recent research has focused on the reactive compatibilization of the blends with maleic anhydride (MAH) grafted copolymers, and the results showed that the MAH grafted copolymers facilitated the improvement of compatibility and mechanical properties of the blends.[9,10] However, the MAH copolymers were found to be corrosive to the equipment during the extruding process. The glycidyl methacrylate copolymers (GMA) showed lower corrosivity to the equipments and could be used as a reactive compatibilizer.[11,12] To our knowledge, the ethylene-acrylate-glycidyl methacrylate copolymer (EAGMA) produced by DuPont has never been used as the compatibilizer in PA 6/ABS blends.

In EAGMA copolymer, there exists a large amount of epoxy groups, which could react with the amine and carboxyl groups in PA 6. The chemical reaction between epoxy groups of EAGMA and amine or carboxyl groups of PA 6 will eventually lead to the formation of EAGMA grafted PA 6 (EAGMA-g-PA 6) copolymer, serving as the compatibilizer in the PA

Correspondence to: B. Huang (huangbf126@126.com).

6/ABS blends. In this article, we are aimed to use EAGMA as the reactive compatibilizer in the PA 6/ABS blend. The mechanism of the reactive compatibilization, the structure, and morphology, as well as the thermal and mechanical properties of the blends was investigated.

EXPERIMENTAL

Materials

Polyamide 6 (PA 6) of intrinsic viscosity of 2.8 dLg^{-1} was provided by the China Petroleum & Chemical Corporation of China (Shanghai, China). Arylonitrile-butadiene-styrene copolymer (ABS) with the grade of 747S was provided by Chi Mei Company of Taiwan (Taipei, Taiwan). Ethylene-acrylate-glycidyl methacrylate copolymer (EAGMA) with the trademark of PTW was purchased from DuPont Company of China (Shanghai, China). The formic acid was purchased from Tianjian Damao Chemical Factory of China (Tianjin, China) and used without further purification.

Blends preparation

The materials of PA 6, ABS, and EAGMA were dried under vacuum at 60°C for 48 h prior to use. The mass ratio of PA 6 to ABS was maintained at 90/10, and the PTW with different mass ratios of 4–28 wt % in 4 wt % increments was added. The materials were mixed by a twin-screw extruder (Nanjing Giant Machinery Co. SHJ-20B) with the temperatures of heating zones 250, 245, 240, 240, 230, and 210°C and the rotating rate of 60 rpm. The extruded pellets were then injected into samples of rectangular shapes of 145 mm in length, 50 mm in width, and 4 mm in thickness, respectively, by the use of an injection molding machine (Shenzhen Bao Gitzo Technology Co., PS610BM). The standard bars were shaped using universal figuring machine (Sans Testing Machine, Shenzhen, China.QJ1000). The samples for the tensile test were shaped to 5-mm-wide dog-bone-shape-strips, with the grip-to-grip distance of 75 mm and the thickness of 4 mm. The samples for the Charpy-notched impact strength test were shaped to bars of 80 mm in length, 10 mm in width, and 4 mm in thickness, respectively, with the notch of one-third of the thickness. The samples for the heat deformation temperature (HDT) test were shaped to bars of 120 mm in length, 10 mm in width, and 4 mm in thickness, respectively.

Solvent extraction

The extruded pellets of the samples (2 g) were added into a flask charged with formic acid (50 mL). After refluxing for 3 days, the residue was taken out and washed with formic acid several times. The residue was then dried in the vacuum oven at 80°C for 2 days to remove the residual formic acid and water for the subsequent characterization.

Measurements

The fourier transform infrared (FTIR) spectra were recorded on a Shimadzu IRPrestige-21 Fourier transform infrared spectrophotometer.

The morphology of the blends was characterized by a FEI Quanta 200 environmental scanning electron microscope (ESEM). The samples were prepared by the treatment of liquid nitrogen, and the fracture surface of the samples was used for observation after gold vapor deposition.

The melting and crystallization behaviors of the samples were investigated by a PYRIS DIAMOND differential scanning calorimeter (DSC) calibrated with indium and zinc standards. The samples of about 5 mg were heated at 260°C for 3 min to erase the thermal history. Then, the samples were cooled to 40°C at a rate of 20°C min^{-1} and subsequently heated to 260°C at a rate of 20°C min^{-1}. The corresponding cooling and heating curves were then recorded, and the corresponding crystallization temperature (T_c), melting temperature (T_m), crystallization enthalpy (ΔH_c), melting enthalpy (ΔH_m) were determined, respectively.

Thermogravimetric analysis (TGA) was performed on a PerkinElmer TGA 7 thermogravimetry at a heating rate of 20°C min^{-1} under nitrogen with a sample size of 8–10 mg. The initial temperature (T_{di}), the temperature at 50 wt % weight loss (T_{50}), the maximum decomposition temperature (T_{max}), as well as the weight loss at 450°C was recorded.

Tensile properties of the samples were determined with a MTS CMT4204 electronic universal test machine (Shenzhen Sans Testing Machine Co., China) at room temperature with a crosshead speed of 60 mm min^{-1}, according to the National Standard of GB/T1040-1992 of China. The Charpy-notched impact strength test was carried out on a XJJD-5 electronic testing machine (Chengde Jinjian Testing Instrument Co., China), according to the National Standard of GB/T1040-1992 of China. Heat deformation temperature (HDT) was measured on a ZFK1302-2 Vicat softening point tester (Jiangdu Tianyuan Instrument Co., China) according to the National Standard of GB/T1634.2-2004 of China.

RESULTS AND DISCUSSION

Structure and morphology

Figure 1 shows the FTIR spectra of ABS, PA 6/ABS and PA 6/ABS/ EAGMA blends, which have been

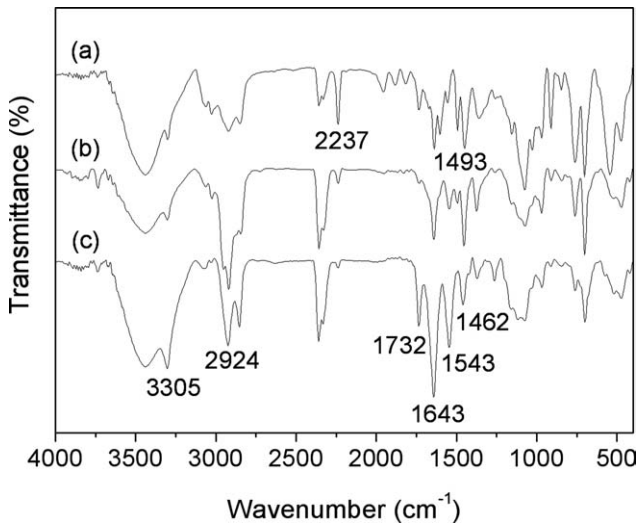

Figure 1 FTIR spectra of (a) pristine ABS and PA 6/ABS blends with (b) 0 wt % and (c) 16 wt % of EAGMA reactive compatibilizer after the treatment of formic acid.

extracted by the formic acid. For the pristine ABS, the characteristic absorption peaks at 2237 and 1493 cm^{-1}, ascribed to nitrile bond and styrene rings are clearly observed. For the PA 6/ABS blend without the addition of EAGMA, the absorption peaks are similar to those of pristine ABS, indicating that the PA 6 component has been completely removed during the extraction process. The blend exhibits additional absorption peaks after the incorporation of EAGMA compatibilizer. The peak at 3305 cm^{-1} is contributed to the N—H stretching vibration, and the peak at 1730 cm^{-1} is attributed to the absorption of carbonyl group. Additionally, the peaks at 2924, 1643, 1543, and 1462 cm^{-1} are ascribed to the C—H asymmetric vibration, the amide I and II band, and C—H deformation vibration, respectively. This indicates that the PA 6 molecular chains remain in the sample after the addition of EAGMA compatibilizer. Furthermore, the absorption at 3441 cm^{-1} in the blend is stronger than that of pristine ABS, suggesting the existence of hydroxyl groups in the blend.

Based on the above results, it is suggested that the PA 6 remains in the blend even after the extraction by formic acid, and PA 6 should be reacted with the EAGMA to form the new copolymers. Otherwise, the pristine PA 6 molecules would be completely removed by formic acid. It is noted that EAGMA contains epoxy groups in the molecular chain, and PA 6 contains carboxyl and amine groups in the molecular chain. During the melt blending, the chemical reaction of the epoxy groups will take place in the presence of carboxyl and amine groups, leading to the formation of EAGMA grafted PA 6 (EAGMA-g-PA 6) copolymers. The mechanism of the reaction is illustrated in Scheme 1. Both carboxyl and amine groups induce the chemical reaction of epoxy groups, and a large amount of hydroxyl groups are produced during the reaction as confirmed by the FTIR analysis. Due to the insolubility of the EAGMA-g-PA 6 copolymer in formic acid, it could not be removed after extraction. The existence of the copolymer might eventually lead to the compatibility between PA 6 and ABS.

In Figure 2, it is observed that the PA 6/ABS blend exhibit the two phase structure in the SEM micrograph. Due to the weak interaction between the two phases, the interface is obvious. The ABS phase is dispersing in the PA 6 matrix in spherical shapes, with some cavities and protrusions produced by fracture after liquid nitrogen treatment. The diameters of the dispersing ABS phase are ranging from about 0.5 to 4 μm. After addition of EAGMA, the fracture surface of the samples shows a significant change, exhibiting a less obvious phase separation. As the EAGMA content is 4 wt %, the ABS phase seems to be uniformly dispersed in the PA 6 matrix, with the diameters of about 0.5 μm. Further increase of the EAGMA content to 12 wt % leads to a better distribution of ABS in PA 6, showing no clear interfaces. The dispersing phase exhibits the diameters of about 0.2 μm. However, the incorporation of excess EAGMA at 16 wt % eventually leads to the appearance of obvious dispersing phase, probably due to the aggregation of the *in situ* formed copolymers.

In comparison with the pristine PA 6/ABS blend, the blends with EAGMA exhibit much smaller dispersing phases. It is suggested that the formation of EAGMA-g-PA 6 copolymers serves as the

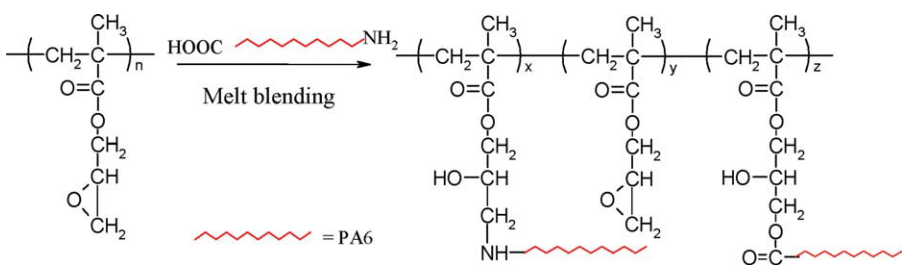

Scheme 1 The formation of compatibilizers by reactive blending [Color figure can be viewed in the online issue, which is available at wileyonlinelibrary.com].

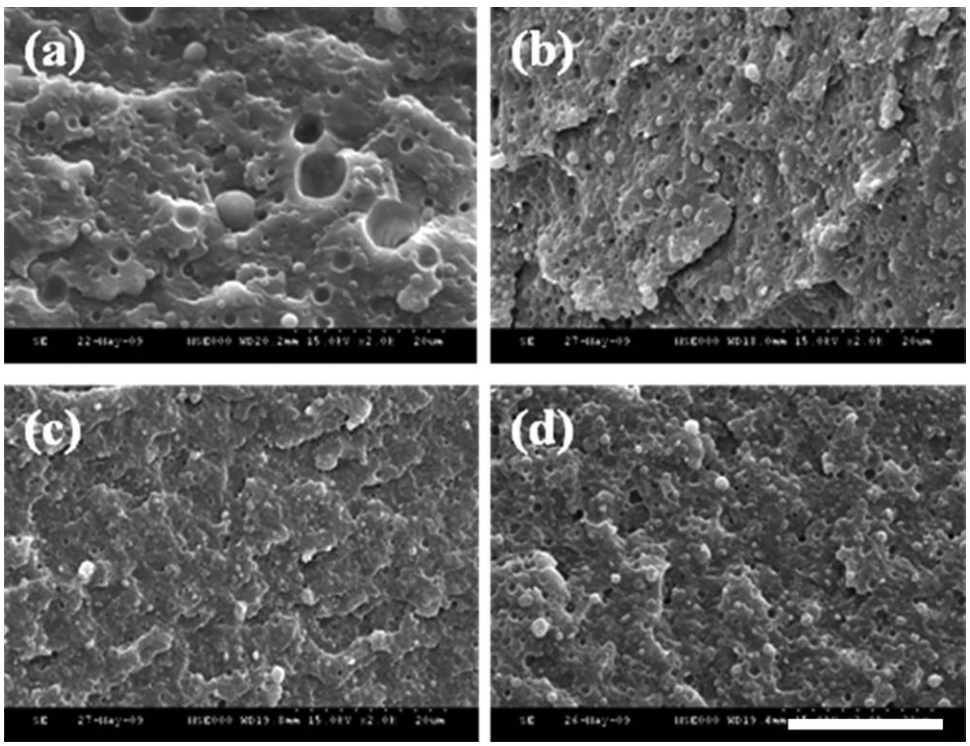

Figure 2 The fracture surface SEM micrographs for PA 6/ABS blends with (a) 0 wt %, (b) 8 wt %, (c) 12 wt %, and (d) 16 wt % of EAGMA reactive compatibilizer, respectively. The scale bar in the micrographs is 20 μm.

compatibilizer, leading to the decrease of interface tension between ABS and PA 6. The distribution of compatibilizers is believed to decrease the diameters of ABS phase in PA 6 matrix. However, too much compatibilizer will aggregate together in the interfaces and form the micelles, leading to the increase of diameters of the ABS dispersing phase.

Thermal properties

The incorporation of EAGMA, as well as the formation of EAGMA-g-PA 6 copolymer, will eventually influence the melting and crystallization behaviors of the PA 6 as shown in Figure 3. During the heating process, both PA 6 and the blends show two main melting peaks [Fig. 3(A)]. The lower melting peak is ascribed to the melting of γ-crystals while the higher melting peak is attributed to the melting of α-crystals of PA 6.[13,14] It is concluded that the incorporation of ABS and EAGMA shows no significant influence on the crystal forms of PA 6. In Figure 3(B), the PA 6 and the blends exhibit a single crystallization peak during the cooling process. The crystallization peak temperature (T_c) of PA 6 shows no significant change with the incorporation of ABS and EAGMA components.

The corresponding data is listed in Table I. It is noted that the PA 6 in the blends exhibits lower crystallization temperature and crystallization enthalpy as compared with pristine PA 6. The incorporation of ABS led to the formation of two phases with ABS distributing in the PA 6 matrix as observed by SEM. The distributing ABS phases interfere with the crystallization of PA 6 probably due to the diluting effect. After the incorporation of 8 wt % EAGMA, the formed EAGMA-g-PA 6 copolymers might distribute in the interfaces of blends, leading to the decrease of diameters of ABS phases. The existence of copolymers may induce the higher crystalline content of PA 6 in the blends, showing a higher crystallization enthalpy value than that of PA 6/ABS blend. Furthermore, the addition of excess EAGMA of 16 wt % leads to the formation of more copolymers, which will eventually form the self-assembled micelles in the interfaces of the blends and show no contribution to the crystallization of PA 6. Therefore, the crystallization enthalpy is lower than the other blends. The crystallization degree (X_c) of PA 6, determined by the crystallization enthalpy, shows a lower value in the blends than pristine PA 6.[14] The corresponding melting enthalpy of the blends is lower than that of pristine PA 6.

The thermogravimetric curves are shown in Figure 4, and the corresponding data is listed in Table II. It is observed that the thermal stability of PA 6 is influenced by the addition of ABS and EAGMA. For the pristine PA 6, the initial temperature to decompose (T_{di}) appears at 370.9°C, in contrast to the T_{di} of PA 6/ABS blend at 364.2°C. However, the

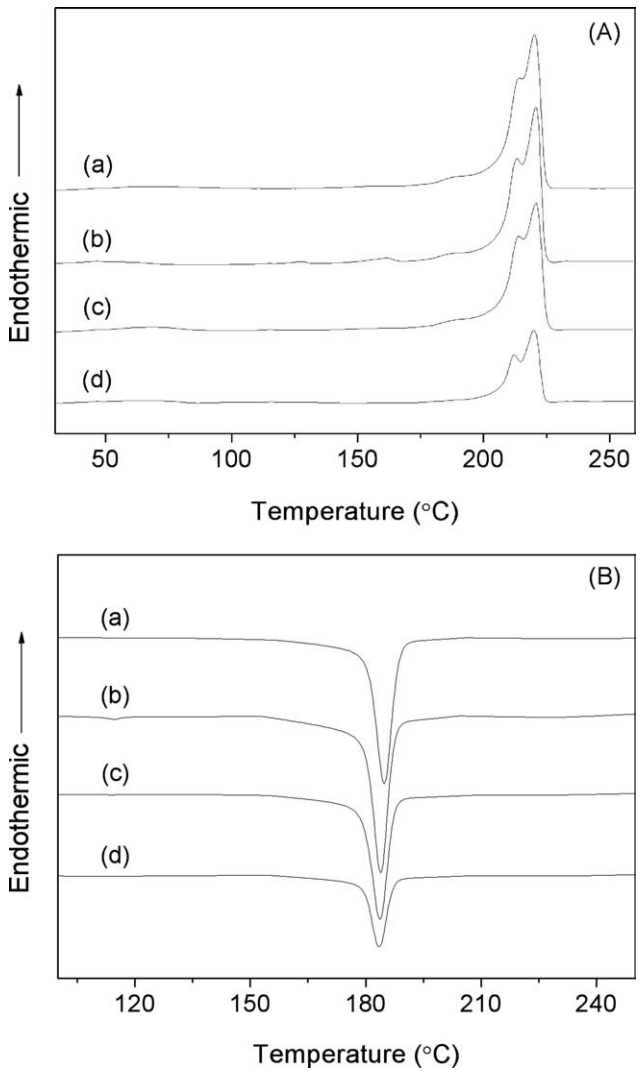

Figure 3 DSC (A) heating and (B) cooling curves for (a) PA 6 and PA 6/ABS blends with (b) 0 wt %, (c) 8 wt %, and (d) 16 wt % of EAGMA reactive compatibilizer, respectively.

incorporation of EAGMA improves the thermal stability of PA 6/ABS blend, showing a T_{di} of 382.2°C. Further increase of the EAGMA content eventually leads to the decrease of T_{di} of the blends. The other kinetic parameters such as T_{50}, T_{max}, and the weight loss at 450°C are also dependent on the EAGMA content, showing the maximum values at EAGMA content of 8 wt %. It is concluded that the incorporation of ABS makes the PA 6 less stable, due to the existence of polybutadiene segment in ABS, which is sensitive to air and heat.

The heat deformation temperature of the blends was also investigated. As shown in Figure 5, the EAGMA content plays the vital role in determining the HDT of PA 6/ABS blends. As the EAGMA content reaches 12 wt %, the blend shows the highest value of HDT, which is about 45°C above the pristine PA 6. However, further increase of the EAGMA content leads to the decrease of HDT value. Based on the TGA result, the HDT values should be also determined by the dispersion of ABS in PA 6 matrix. The good dispersion of ABS in PA 6 matrix leads to the small dispersing phase, facilitating the crystallization of PA 6 and improvement of the thermal stability of the blends. The addition of excess EAGMA facilitates the aggregation of copolymers and formation of micelles in the interfaces of the blends, which eventually deteriorates the crystallization of PA 6 and decreases the thermal stability of the blends.

Mechanical properties

The mechanical properties of the blends were investigated as shown in Figure 6. It is noted that the tensile strength of the samples decreases as the EAGMA content increases. Additionally, the tensile strength exhibits a sharp decrease as the EAGMA content increases from 8 to 12 wt %. In comparison, the impact strength of the samples increases with increasing EAGMA content. The impact strength of the blends reaches the highest value of 15.5 kJ m^{-2} after addition of 20 wt % EAGMA, which is about 323% of the pristine PA 6.

The tensile strength reflects the values of external force causing segmental movement of the polymer chains.[15] The incorporation of EAGMA compatiblizer led to the decrease of crystallinity of PA 6. In addition, the formed EAGMA-g-PA 6 copolymers distribute in the interface of PA 6 and ABS phases, leading to the formation of transition layer. The existence of the transition layer facilitates the stress transfer between the PA 6 and ABS phases, resulting in the easier movement of the polymer segments under external forces. Therefore, the tensile strength of the blends decreases due to the decreased crystallinity of PA 6 and easy movement of the polymer segments.

TABLE I
DSC Data for PA 6/ABS Blends with Different Content of EAGMA Compatibilizers

PA 6/ABS/EAGMA	T_c (°C)	T_{m1} (°C)	T_{m2} (°C)	ΔH_c (J/g)	ΔH_m (J/g)	X_c (%)
100/0/0	184.9	214.0	220.0	61.8	52.4	27.4
90/10/0	183.9	213.0	220.6	56.6	46.8	24.5
82.8/9.2/8.0	183.8	214.0	220.6	59.3	50.5	26.4
75.6/8.4/16.0	183.5	212.0	219.6	50.5	46.4	24.3

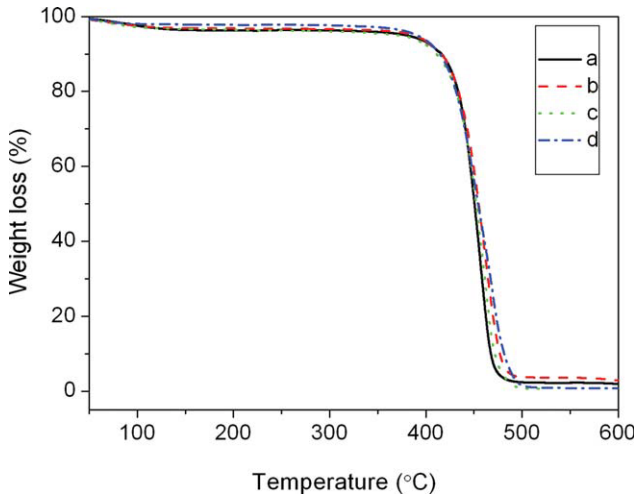

Figure 4 TGA curves for PA 6/ABS blends with (a) 0 wt %, (b) 8 wt %, (c) 12 wt %, and (d) 16 wt % of EAGMA reactive compatibilizer, respectively [Color figure can be viewed in the online issue, which is available at wileyonlinelibrary.com].

The impact strength is believed to be dependent on the morphology of the blends. The decrease in diameters of the dispersing phase results in the improvement of impact strength, accounting for the strong interfacial adhesion between PA 6 and ABS. However, too much EAGMA will eventually lead to the formation of micelles in the interfaces, resulting in the weak interactions between the phases and the failure of cavitation of ABS particles.

CONCLUSIONS

The PA 6/ABS blends compatibilized by EAGMA were successfully prepared via twin-screw extrusion. The EAGMA was confirmed to react with PA 6 to form the EAGMA-g-PA 6 copolymer via the ring-opening reaction in the presence of amine and carboxyl groups during the blending process. The EAGMA significantly improved the dispersion of ABS phase in PA 6 matrix, and the diameters of ABS phase were dependent on the content of

TABLE II
TGA Kinetic Parameters for PA 6/ABS Blends with Different Content of EAGMA Compatibilizers

PA 6/ABS/EAGMA	T_{di}[a] (°C)	T_{50}[b] (°C)	Weight loss at 450°C (wt %)	T_{max}[c] (°C)
100/0/0	370.9	455.0	49.0	460.8
90/10/0	364.2	450.6	40.9	456.2
82.8/9.2/8.0	382.2	454.2	45.8	468.8
75.6/8.4/16.0	371.9	452.2	43.5	463.4

[a] The initial decomposition temperature of the blends.
[b] The temperature at 50 wt % weight loss of the blends.
[c] The maximum decomposition temperature of the blends.

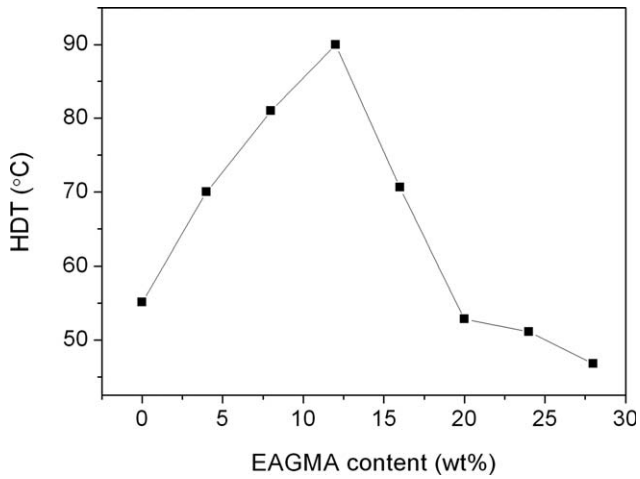

Figure 5 Heat deformation temperature for PA 6/ABS blends versus EAGMA content.

EAGMA. The blends exhibited double melting peaks ascribing for the melting of γ- and α-crystals, and the EAGMA showed no significant effect on the crystal form of PA 6. The incorporation of EAGMA at low content improved the thermal stability of blends. Further increase of the EAGMA content led to the decomposition of the blends at lower temperatures. Heat deformation temperature of the blends was dependent on the EAGMA content, showing the maximum value at EAGMA content of 12 wt %, which is about 45°C higher than the pristine PA 6. The tensile strength decreased with increasing EAGMA content due to the low crystallinity of PA 6 and weak interfacial interaction. Correspondingly, the impact strength of the blends exhibited the highest value of 15.5 kJ m^{-2} at EAGMA content of 20 wt %, which is about 323 % of pristine PA 6. The EAGMA is recognized to be an effective compatibilizer for the PA 6 based blends via reactive compatibilization.

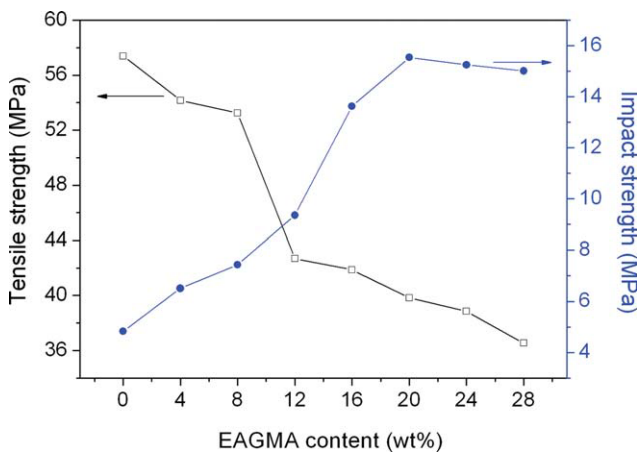

Figure 6 Tensile strength and impact strength for PA 6/ABS blends versus EAGMA content [Color figure can be viewed in the online issue, which is available at wileyonlinelibrary.com].

References

1. Manning, S. C.; Moore, R. B. Polym Eng Sci 1999, 39, 1921.
2. Huang, J. W.; Chang, C. C.; Kang, C. C.; Yeh, M. Y. Thermochim Acta 2008, 468, 66.
3. Wilkinson, A. N.; Clemens, M. L.; Harding, V. M. Polymer 2004, 45, 5239.
4. Liu, N. C.; Xie, H. Q.; Baker, W. E. Polymer 1993, 34, 4680.
5. Wang, C.; Su, J. X.; Li, J.; Yang, H.; Zhang, Q.; Du, R. N.; Fu, Q. Polymer 2006, 47, 3197.
6. Kudva, R. A.; Keskkula, H.; Paul, D. R. Polymer 1998, 39, 2447.
7. Ju, M. Y.; Chang, F. C. Polymer 2000, 41, 1719.
8. Zhang, C.; Dai, G. J Mater Sci 2007, 42, 9947.
9. Chow, W. S.; Mohd Ishak, Z. A.; Karger-Kocsis, J.; Apostolov, A. A.; Ishiaku, U. S. Polymer 2003, 44, 7427.
10. Arone, E. J.; Kopcak, U.; Goncalves, M. C.; Nunes, S. P. Polymer 2000, 41, 5929.
11. Zhang C.; Dai, G. J Mater Sci 2007, 42, 9947.
12. Chiono, V.; Filippi, S.; Yordanov, H.; Minkova, L.; Magagnini, P. Polymer 2003, 44, 2423.
13. Sallem-Idrissi, N.; Miri, V.; Elkoun, S.; Krawczak, P.; Lacrampe, M. F.; Lefebvre, J. M.; Seguela, R. Polymer 2009, 50, 5812.
14. Lai, S. M.; Li, H. C.; Liao, Y. C. Eur Polym J 2007, 43, 1660.
15. Stachurski, Z. H. Prog Polym Sci 1997, 22, 407.